

# Specific Alleles of *CLN7/MFSD8*, a Protein That Localizes to Photoreceptor Synaptic Terminals, Cause a Spectrum of Nonsyndromic Retinal Dystrophy

Kamron N. Khan,<sup>1-4</sup> Mohammed E. El-Asrag,<sup>3,5</sup> Cristy A. Ku,<sup>6</sup> Graham E. Holder,<sup>1,2,7</sup> Martin McKibbin,<sup>3,4</sup> Gavin Arno,<sup>1</sup> James A. Poulter,<sup>3</sup> Keren Carss,<sup>8,9</sup> Tejaswi Bommireddy,<sup>4</sup> Saghar Bagheri,<sup>10</sup> Benjamin Bakall,<sup>11,12</sup> Hendrik P. Scholl,<sup>10</sup> F. Lucy Raymond,<sup>8,13</sup> Carmel Toomes,<sup>3</sup> Chris F. Inglehearn,<sup>3</sup> Mark E. Pennesi,<sup>6</sup> Anthony T. Moore,<sup>1,2,14</sup> Michel Michaelides,<sup>1,2</sup> Andrew R. Webster,<sup>1,2</sup> and Manir Ali<sup>3</sup>; for NIHR BioResource-Rare Diseases and UK Inherited Retinal Disease Consortium

<sup>1</sup>University College London Institute of Ophthalmology, London, United Kingdom

<sup>2</sup>Inherited Eye Disease Service, Moorfields Eye Hospital, London, United Kingdom

<sup>3</sup>Section of Ophthalmology and Neuroscience, Leeds Institute of Biomedical and Clinical Sciences, University of Leeds, St. James's University Hospital, Leeds, United Kingdom

<sup>4</sup>Department of Ophthalmology, St. James's University Hospital, Leeds, United Kingdom

<sup>5</sup>Department of Zoology, Faculty of Science, Benha University, Benha, Egypt

<sup>6</sup>Casey Eye Institute, Oregon Health & Science University, Portland, Oregon, United States

<sup>7</sup>Department of Electrophysiology, Moorfields Eye Hospital, London, United Kingdom

<sup>8</sup>National Institute for Health Research BioResource-Rare Diseases, Cambridge University Hospitals, Cambridge Biomedical Campus, Cambridge, United Kingdom

<sup>9</sup>Department of Haematology, University of Cambridge, Cambridge, United Kingdom

<sup>10</sup>Wilmer Eye Institute, Johns Hopkins University, Baltimore, Maryland, United States

<sup>11</sup>Associated Retina Consultants, Phoenix, Arizona, United States

<sup>12</sup>University of Arizona, College of Medicine, Phoenix, Arizona, United States

<sup>13</sup>Department of Medical Genetics, Cambridge Institute for Medical Research, University of Cambridge, Cambridge, United Kingdom

<sup>14</sup>Department of Ophthalmology, University of California-San Francisco School of Medicine, San Francisco, California, United States

Correspondence: Manir Ali, Section of Ophthalmology and Neuroscience, Leeds Institute of Biomedical and Clinical Sciences, University of Leeds, Leeds LS9 7TF, UK; medma@leeds.ac.uk.

Kamron N. Khan, Medical Retina Service, Moorfields Eye Hospital, 162 City Road, London EC1V 2PD, UK; kamron.khan@moorfields.nhs.uk.

See the appendix for the members of the NIHR BioResource-Rare Diseases and UK Inherited Retinal Disease Consortium.

KNK and MEE contributed equally to the work presented here and should therefore be regarded as equivalent first authors.

MM, ARW, and MA contributed equally to the work presented here and should therefore be regarded as equivalent senior authors.

Submitted: August 24, 2016

Accepted: March 14, 2017

Citation: Khan KN, El-Asrag ME, Ku CA, et al.; for NIHR BioResource-Rare Diseases and UK Inherited Retinal Disease Consortium. Specific alleles of *CLN7/MFSD8*, a protein that localizes to photoreceptor synaptic terminals, cause a spectrum of nonsyndromic retinal dystrophy. *Invest Ophthalmol Vis Sci.* 2017;58:2906-2914. DOI:10.1167/iovs.16-20608

**PURPOSE.** Recessive mutations in *CLN7/MFSD8* usually cause variant late-infantile onset neuronal ceroid lipofuscinosis (vLINCL), a poorly understood neurodegenerative condition, though mutations may also cause nonsyndromic maculopathy. A series of 12 patients with nonsyndromic retinopathy due to novel *CLN7/MFSD8* mutation combinations were investigated in this study.

**METHODS.** Affected patients and their family members were recruited in ophthalmic clinics at each center where they were examined by retinal imaging and detailed electrophysiology. Whole exome or genome next generation sequencing was performed on genomic DNA from at least one affected family member. Immunofluorescence confocal microscopy of murine retina cross-sections were used to localize the protein.

**RESULTS.** Compound heterozygous alleles were identified in six cases, one of which was always p.Glu336Gln. Such combinations resulted in isolated macular disease. Six further cases were homozygous for the variant p.Met454Thr, identified as a founder mutation of South Asian origin. Those patients had widespread generalized retinal disease, characterized by electroretinography as a rod-cone dystrophy with severe macular involvement. In addition, the photopic single flash electroretinograms demonstrated a reduced b- to a-wave amplitude ratio, suggesting dysfunction occurring after phototransduction. Immunohistology identified MFSD8 in the outer plexiform layer of the retina, a site rich in photoreceptor synapses.

**CONCLUSIONS.** This study highlights a hierarchy of *MFSD8* variant severity, predicting three consequences of mutation: (1) nonsyndromic localized maculopathy, (2) nonsyndromic widespread retinopathy, or (3) syndromic neurological disease. The data also shed light on the underlying pathogenesis by implicating the photoreceptor synaptic terminals as the major site of retinal disease.

**Keywords:** macular degeneration, retinal dystrophy, DNA sequencing, electroretinography, immunohistology, photoreceptor synapse



Inherited retinal dystrophies (IRD) are a complex group of genetically heterogeneous eye disorders that are caused by Mendelian mutations in over 200 genes (see <https://sph.uth.edu/retnet/>; provided in the public domain by The University of Texas Health Science Center, Houston, TX, USA). They are initially diagnosed according to the patient's clinical symptoms, their age of onset, and the cell type that is primarily affected by the condition. Knowledge of the underlying genetic defect allows for a more comprehensive description, though the assumption that each genetic disorder may have a unique clinical signature is oversimplified since molecular screening has revealed profound heterogeneity, both clinical and genetic, in inherited retinal diseases. Additionally, we are now starting to appreciate that isolated retinal disease can be associated with variants in genes previously identified as only causing syndromic disease.<sup>1</sup>

The neuronal ceroid lipofuscinoses (NCLs) are a group of lysosomal storage disorders resulting from single gene defects in lysosomal hydrolases or lysosomal/endoplasmic reticulum membrane proteins.<sup>2</sup> They are characterized by early onset neurodegeneration associated with accumulation of autofluorescent intracellular inclusions in neurons and extraneuronal tissues.<sup>3</sup> Collectively, they are the most common cause of childhood neurodegenerative disease. Initially classified using clinical and electron microscopic features, the NCLs are now defined primarily by their genetic basis. At least 13 genetic forms are currently recognized (*CLN1-8* and *CLN10-14*); with the exception of *CLN4* disease, all are recessively inherited.

Mutations in the major facilitator superfamily (MFS) domain-containing protein 8 (*MFSD8/CLN7*, MIM 611124) were found to cause a variant of late-infantile NCL (vLINCL, MIM 610951).<sup>4-8</sup> Symptoms of vLINCL usually start between the ages of 3 and 6 years, with seizures and developmental regression followed by speech failure, ataxia, visual loss, myoclonus, and ultimately premature death. Recently, recessive mutations in *MFSD8* have also been associated with nonsyndromic macular dystrophy in two families.<sup>9</sup> Retinal dysfunction in the absence of syndromic association had not previously been reported. Despite many advances in NCL research, the biological basis for neurodegeneration remains elusive. The present study provides novel mechanistic insights gleaned from detailed phenotypic investigations in 12 patients with *MFSD8*-associated retinopathy, together with immunolocalization studies in the murine retina. Possible genotype-phenotype correlations underlying nonsyndromic and syndromic disease are also discussed.

## MATERIALS AND METHODS

### Patient Ascertainment and Clinical Evaluation

The study was approved by the appropriate local research ethics committees and the protocol adhered to the tenets of the Declaration of Helsinki. Patients were ascertained from the inherited eye disease clinics at Moorfields Eye Hospital, London (Patients GC19741, GC17967, GC14328, GC18458, GC19832, GC3716, and GC4694), Bradford Royal Infirmary, Bradford (Patient LE1), St. James's University Hospital, Leeds (Patients LE2 and LE3), Casey Eye Institute, Portland (CEI1), and Wilmer Eye Institute, Baltimore (CEI2). A diagnosis of inherited retinal disease was made by an experienced ophthalmologist based on signs and symptoms, including progressive and symmetrical retinal disease.

Detailed clinical investigations included best-corrected visual acuity (VA; Snellen chart), confrontation visual fields, and pattern and full-field electroretinography (PERG, ERG) using techniques that incorporated the International Society of

Clinical Electrophysiology of Vision (ISCEV) recommendations.<sup>10,11</sup> Retinal imaging was performed using color fundus photography (Topcon TRC 501A retinal camera, Topcon Corp., Tokyo, Japan), spectral-domain optical coherence tomography (Spectralis HRA+OCT, Heidelberg Engineering, Heidelberg, Germany), and 488-nm wavelength fundus autofluorescence (AF) with either a 30° or 55° field (Spectralis HRA+OCT, Heidelberg Engineering).

### Molecular Genetic Analysis

Genomic DNA from affected patients was extracted and analyzed either by whole exome (SureSelect All Exon XT Sequencing kit, Agilent Technologies, Santa Clara, CA, USA) or by whole genome sequencing (Illumina TruSeq DNA PCR-free sample preparation kit, Illumina, San Diego, CA, USA, followed by Illumina HiSeq 2500 sequencing as part of the NIH Rare BioResource-Rare Diseases project) according to the manufacturer's instructions. FastQ files were aligned to the GRCh37 (hg19) reference genome. Potentially pathogenic variants were identified, filtered based on functionality, minor allele frequency (MAF) in public and in-house databases, and on calculated pathogenicity scores. Putative mutations were validated by Sanger sequencing and checked for segregation.

### Immunofluorescence and Confocal Microscopy

Sagittal sections from the eyes of 30-day-old mice were incubated with goat polyclonal anti-MFSD8 (S-14; Santa Cruz Biotechnology, Heidelberg, Germany), followed by an Alexa Fluor 568-conjugated donkey anti-goat immunoglobulin (Molecular Probes, Inc., Eugene, OR, USA). Nuclei were counterstained with DAPI (Vector Laboratories, Orton Southgate, UK). As controls, a section was stained with secondary and another was treated with primary antibody that had been preincubated with peptide antigen followed by secondary. For the colocalization experiments, sections were incubated with anti-MFSD8 and either rabbit polyclonal anti-SNAP-25 (ab5666; Abcam, Cambridge, UK) or rabbit polyclonal anti-PSD-95 (ab18258; Abcam) followed by Alexa Fluor 568-conjugated donkey anti-goat immunoglobulin and Alexa Fluor 488-conjugated chicken anti-rabbit immunoglobulin (Molecular Probes, Inc.), and counterstained with DAPI. Confocal images were obtained using an Eclipse TE2000-E system microscope (Nikon Corp., Tokyo, Japan) and processed using Nikon EZ-C1 3.50 software.

## RESULTS

### Molecular Analysis

Nine families were identified by next generation sequencing of genomic DNA from patients with nonsyndromic retinal dystrophy, which included 12 individuals carrying biallelic variants in *MFSD8* (Fig. 1). Six of the cases (GC19741, LE1-LE3, CEI1, and CEI2) were compound heterozygotes that carried the variant, c.1006G>C, p.Glu336Gln, paired with one of three other disease-causing alleles. This allele was identified in trans with a null variant (c.103C>T, p.Arg35Ter for GC19741 or c.233G>A, p.Trp78Ter for CEI1 and CEI2) or a missense change (c.1394G>A, p.Arg465Gln for LE1-LE3). The remaining six cases (GC17967, GC14328, GC18458, GC19832, GC3716, and GC4694) were homozygous for the missense variant, c.1361T>C, p.Met454Thr. Three of these individuals (GC17967, GC14328, and GC3716) were the offspring of three separate consanguineous marriages. A common shared founder haplotype of South Asian origin, spanning approximately 1.47 Mb was identified by examining single nucleotide variants in

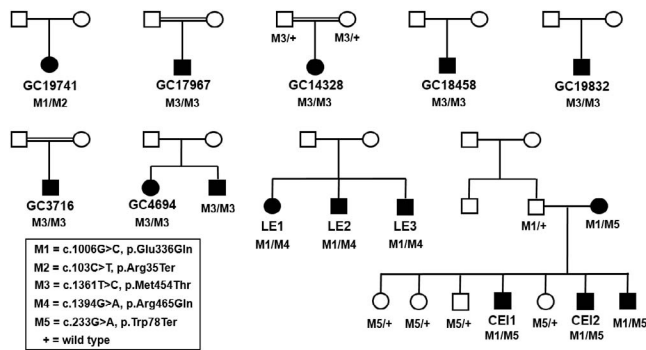


**FIGURE 1.** Families and case subjects reported in this study and *MFSD8* mutation data. The affected patients (*shaded black*) who were examined are shown with their identification code (GC19741, GC17967, GC14328, GC18458, GC19832, GC3716, GC4694, LE1-LE3, CEI1, and CEI2). The genotypes for all subjects tested are shown below each individual, with M representing the mutant allele as shown and + representing the wild-type allele.

the WGS data at the *MFSD8* locus from four cases with the homozygous variant c.1361T>C (Supplementary Table S1). The variants were found to co-segregate with the disease in all family members from whom DNA was available (Fig. 1).

### Clinical Investigations

The clinical features of the 12 cases are summarized in the Table. Central visual loss was the primary complaint in all patients. Patients with isolated maculopathy (GC19741, LE1-LE3, CEI1, and CEI2) developed symptoms at a later age than those with generalized retinopathy (GC17967, GC14328, GC18458, GC19832, GC3716, and GC4694). Patients with a compound heterozygous genotype that included c.1006G>C, p.Glu336Gln had isolated macular disease. In contrast, cases with a homozygous c.1361T>C, p.Met454Thr genotype had more widespread retinopathy, with the majority also reporting night-blindness. No signs or symptoms of neurological disease were apparent. Fundus examination findings ranged from minimal changes (GC19741) to those typical of advanced retinitis pigmentosa (GC3716; Fig. 2A). Corresponding structural changes were present in all cases when imaged using AF and optical coherence tomography (OCT; Figs. 2B, 2C).

Patients with clinically isolated macular disease (CEI1 and GC19741) initially showed only pattern ERG abnormalities, though as the disease progressed the full field ERG could become abnormal, with the photopic single flash ERG (CEI1) showing a disproportionate loss of b- to a-wave leading to a significantly reduced b- to a-wave ratio (Fig. 3). Patients with peripheral retinal signs (GC17967 and GC14328) also had highly abnormal full-field ERGs, in keeping with a severe rod-cone dystrophy with marked macular involvement (Fig. 3). The photopic single flash ERGs (GC17967 and GC14328) again showed reduction in the b to a amplitude ratio. Although there was a lower amplitude b-wave than a-wave in the bright flash dark-adapted ERG, that is likely to be a reflection of a cone isolated retina, with all signals arising from dark-adapted cones, rather than inner retinal dysfunction with the rod system.

### CLN7/MFSD8 Localization in the Retina

Confocal immunofluorescence microscopy in the murine retina showed that *MFSD8* predominantly localized to the outer plexiform layer (OPL), a region rich in synaptic connections between photoreceptors and second order neurons—bipolar and horizontal cells (Fig. 4). Co-localization

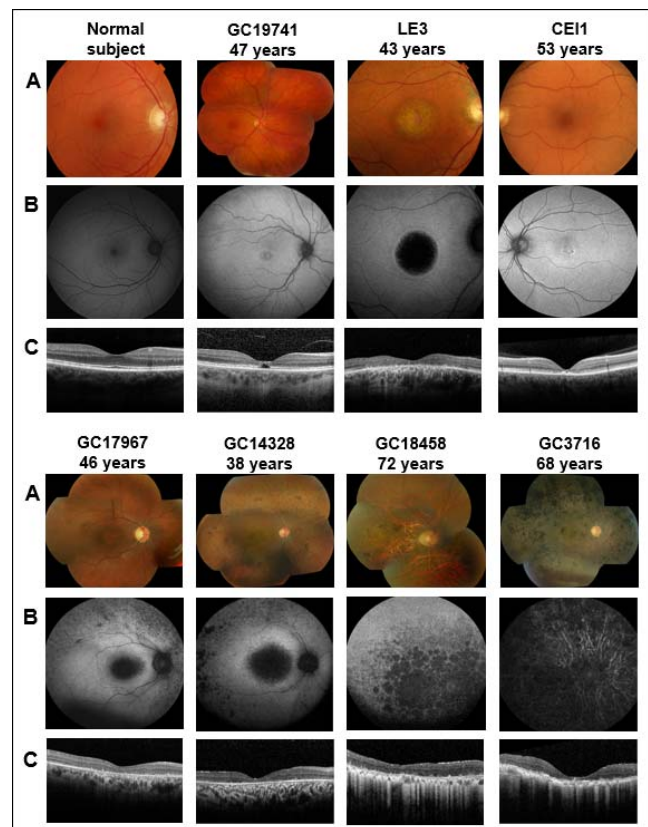


**FIGURE 2.** Retinal images of patients with nonsyndromic retinal dystrophy caused by biallelic *MFSD8* mutations. Color fundus photographs (CFPs) (A), 488-nm fundus autofluorescence (FAF) images (B), and macular OCT scans (C) from patients GC19741, LE3, CEI1, GC17967, GC14328, GC18458, GC3716, and a normal control subject. GC19741 and CEI1 have disease that is localized to the fovea, with minimal if any signs visible on CFPs. The subtle increase in foveal AF correlates with the outer retinal cavitation on OCT suggesting focal loss of photoreceptors. LE3 manifests a more severe maculopathy. GC17967, GC14328, GC18458, and GC3716 show more extensive disease typical of retinitis pigmentosa with severe macular involvement. Imaging shows pigment migration into the retina and arteriolar attenuation (CFP), and loss of physiological AF, consistent with extensive degeneration of the outer retinal structures (FAF and OCT). GC14328 additionally manifests a ring of increased AF demarcating the central boundary between normal and abnormal retina; in GC3716 the atrophy is so advanced that choroidal vessel AF is visible.

studies highlighted considerable overlap in the staining pattern for *MFSD8* localization and PSD-95, but not SNAP-25, suggesting that *MFSD8* is predominantly located at the photoreceptor synaptic terminals rather than bipolar or horizontal cells.

### DISCUSSION

Mutations in *MFSD8* usually cause vLINCL, a severe, early-onset neurodegeneration characterized by seizures, progressive mental and motor deterioration, myoclonus, visual failure, and ultimately premature death.<sup>4-8,14-19</sup> Atypical presentations also exist, either commencing at a later age associated with mild disease,<sup>7</sup> or a recently described, nonsyndromic form causing only macular disease.<sup>9</sup> The present study describes a fourth consequence of *MFSD8* dysfunction: widespread rod-cone dystrophy with severe macular involvement. Longitudinal study is needed to determine whether patients with isolated retinal disease eventually develop neurological involvement,

TABLE. Clinical Information of Retinal Dystrophy Patients With Biallelic MFSD8 Mutations Identified in This Study

Patient ID	GC19741	GC17967	GC14328	GC18458	GC19832	GC3716	GC4694	LE1	LE2	LE3	CEI1	CEI2
Ethnicity	English	Turkish	South Indian	Western Indian (Gujarati)	South Indian	Tamil	Indian	English	English	English	European/Native American	European/Native American
Age of onset	46	Early 30s	19	Early 20s	26	30s	20s	30	28	Early 30s	35	28
Symptoms	+	+	++	++	++	++	++	+	+	+	+	+
Loss of acuity	-	-	+	+	+	+	+	-	-	-	-	-
Nyctalopia	6/36, 6/18	6/36, 6/36	6/24, 6/60	6/36, 6/18	6/24, 6/24	6/60, 6/60	1/60, 1/60	6/18, 6/18	6/9, 6/18	6/36, 6/60	2/5, 2/5	4/25, 1/8
Presentation BCVA (Snellen)	6/60, 6/48	3/60, 3/60	6/60, 4/60	CF, HM	6/24, 6/24	NPL, PL	HM, HM	6/60, 6/60	6/36, 6/60	6/60, 6/60	1/5, 1/10	1/5, 1/10
Follow up, y	3	10	12	42	3	23	13	4	16	1	5	10
Refraction, MSE	nd	nd	nd	-7D	-5D	nd	nd	-1D	-1D	-3D	nd	nd
Neurology, age at last examination	Normal (51)	Normal (47)	Normal (39)	Normal (71)	Normal (38)	Normal (78)	Normal (66)	Normal (47)	Normal (44)	Normal (43)	Normal (54)	Normal (49)
Working diagnosis	Occult macular dystrophy	arRCD	arRCD	arRCD	arRCD	arRCD	arRCD	arMD	arMD	arMD	Occult macular dystrophy	arMD
Electrophysiology	Central macular dysfunction only	Severe rod-cone dystrophy. Undetectable PERG	Severe rod-cone dystrophy. Undetectable PERG	Abnormal photopic and scotopic ERG (Age 29)	Central macular dysfunction. Very mild rod and cone dysfunction (Age 35)	nd	nd	Central macular dysfunction only	Central macular dysfunction only	nd	Central macular dysfunction only	Central macular dysfunction only
CFP												
Macular atrophy	Loss of foveal reflex	+	+	+	+	+	+	+	+	+	Altered foveal reflex only	+
Peripheral pigmentation	-	+	+	+	-	+	+	-	-	-	-	-
AF												
Central hypo-AF	Initially hyper-AF with later loss of AF	+	+	+	+	+	+	+	nd	+	Initially hyper-AF with later loss of AF	+
Ring hyper-AF	-	+	+	+	-	-	-	+	nd	+	+	+
Peripheral hypo-AF	-	+	+	+	-	+	+	nd	nd	-	-	-
OCT												
Macular atrophy	+	+	+	+	+	+	+	+	+	+	+	+
Other	Loss POS, preservation of the ELM, then progressive atrophy			Choroidal atrophy		Choroidal atrophy, INL/ONL cysts	Choroidal atrophy, INL/ONL cysts				Loss POS, preservation of the ELM, then progressive atrophy	
Mutation												
c.103C>T, p.Arg357Ile								c.1006G>C, p.Glu336Gln				c.233G>A, p.Trp78Ile
c.1006G>C, p.Glu336Gln		c.1361T>C, p.Met454Thr						c.1394G>A, p.Arg465Gln				c.1006G>C, p.Glu336Gln

+, present; -, absent; arMD, autosomal recessive macular dystrophy; arRCD, autosomal recessive rod-cone dystrophy; BCVA, best-corrected visual acuity; CFP, color fundus photography; D, diopter; ELM, external limiting membrane; INL, inner nuclear layer; MSE, mean spherical equivalent; nd, not done; ONL, outer nuclear layer; POS, photoreceptor outer segments.

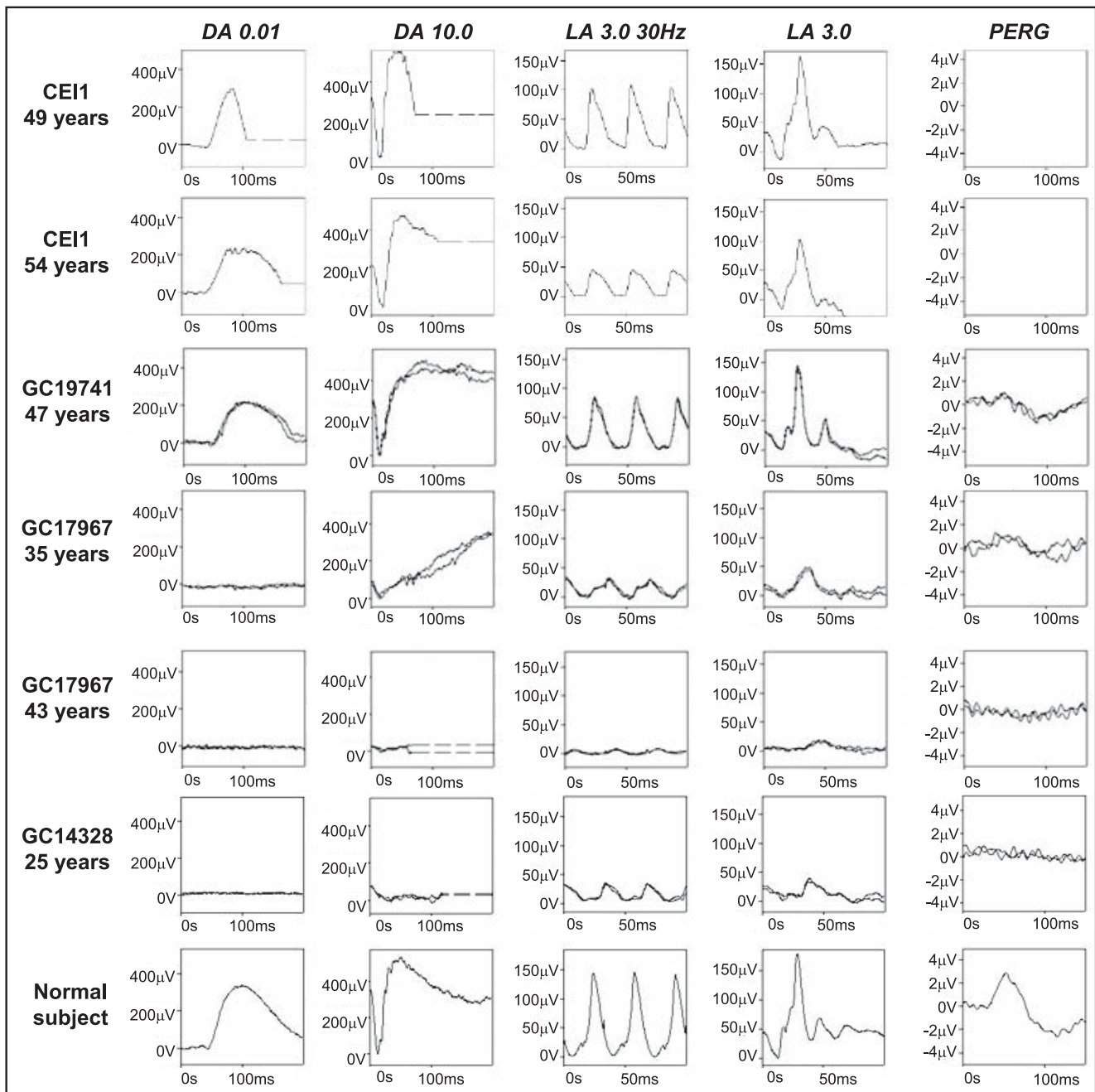


**FIGURE 3.** ERG and PERG of four patients (CEI1, GC19741, GC17967, and GC14328) and a normal subject. The ages of the subjects at examination are shown. The ISCEV standard ERGs, with conventional nomenclature, are shown. DA, dark-adapted; LA, light-adapted. The subsequent number indicates flash strength in  $\text{cd.s.m}^{-2}$ . All are single flash responses other than the LA 30-Hz response, which uses computerized signal averaging. Blink artefact in CEI1 (at 49 and 54 years), GC17967 (at 43 years), and GC14328 has been replaced by broken lines. CEI1 and GC19741, who have a macular dystrophy phenotype, show normal full-field ERGs (for initial CEI1 and GC19741 recordings) but a subnormal PERG (when available). The later recording of CEI1 shows a normal dark-adapted response but a reduced b- to a-wave ratio in the LA 3.0 response in keeping with a progressive loss of inner retinal cone function. The initial recordings of GC17967 show marked loss of rod system function with generalized cone system dysfunction. The DA 0.01 response is undetectable, the DA 10.0 shows a markedly abnormal a-wave in keeping with photoreceptor dysfunction, LA 3.0 30 Hz and LA 3.0 are subnormal and markedly delayed, and the PERG is detectable but subnormal. These findings indicate a rod-cone dystrophy with relatively mild macular involvement. Later recordings show an undetectable PERG in keeping with worsening macular function, and all detectable ERGs show profound deterioration. GC14328 and the later recordings of GC17967 show a lower b- than a-wave in the DA 10.0 response suggesting a dark-adapted cone origin with all rod function having been lost. The photopic ERGs are subnormal and delayed, but over time there is the development of a broadened a-wave in the LA 3.0 response with marked reduction in the b to a ratio in keeping with additional inner retinal cone system dysfunction. The recordings from a normal control subject are included for comparison.

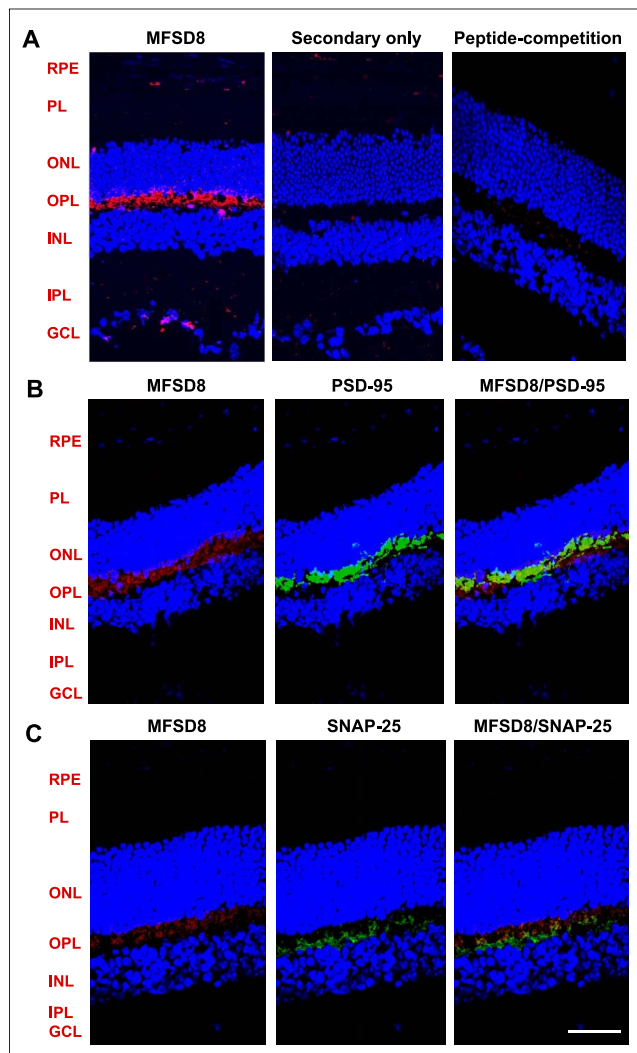


**FIGURE 4.** Localization of MFSD8 to the OPL. Immunofluorescence photomicrographs of mouse retinal sagittal sections stained with anti-MFSD8 only (A), or combined with anti-PSD-95 (B) or anti-SNAP-25 (C) and Alexa Fluor 568-conjugated secondary antibody (red) or Alexa Fluor 488-conjugated secondary antibody (green) and DAPI nuclear counterstain (blue) are shown. The secondary antibody alone or anti-MFSD8 preincubated with peptide were incubated with different serial sections as controls in the experiment. The images shown in B and C are separate and merged channels of the same section. The layers of the retina are depicted; retinal pigment epithelium (RPE), photoreceptor layer (PL), outer nuclear layer (ONL), OPL, inner nuclear layer (INL), inner plexiform layer (IPL), and the ganglion cell layer (GCL) are shown. Scale bar represents 50  $\mu\text{m}$ . Note that MFSD8 staining predominantly co-localizes with PSD-95, a known marker for presynaptic photoreceptor terminals.<sup>12</sup> SNAP-25 localizes to horizontal cells at the OPL.<sup>13</sup>

though it is reassuring that the three oldest patients reported herein developed no neurological abnormalities despite being in their seventh or eighth decade of life.

ERG localizes the consequences of MFSD8 dysfunction more precisely. The scotopic bright flash ERG is a mixed rod-cone response, dominated by the rod-system. Most of the negative going a-wave reflects photoreceptor hyperpolarization, with the later positive going b-wave generated in the bipolar cells. The photopic single flash ERG a-wave is generated by cone photoreceptors and Off-(hyperpolarizing) bipolar cells, with the positive b-wave being an effectively

synchronized response from On- and Off-bipolar cells. Those patients homozygous for the p.Met454Thr allele demonstrated a reduction in the photopic b to a ratio, a feature not typically associated with primary photoreceptor degeneration. Although a reduced b- to a-wave ratio can occur in the bright flash dark-adapted ERG in cone isolated retinas due to vitamin A deficiency,<sup>20</sup> or RDH5 mutation,<sup>21</sup> when rod loss is so severe that all remaining signals arise in dark-adapted cones, the photopic ERGs do not exhibit such a phenomenon. The reduced photopic b to a ratio in the present series thus indicates dysfunction after phototransduction beyond the photoreceptor outer segment. This contention is further supported in a patient carrying the p.Glu336Gln variant allele, who has isolated macular disease but developed a reduced photopic ERG b- to a-wave ratio over a 6-year period, indicating progressive “inner retinal” cone dysfunction. Immunofluorescence of the murine retinal sections demonstrated that the strongest MFSD8 signal arises in the OPL, in the photoreceptor synaptic terminals, in keeping with the electrophysiological data.

Thus two independent lines of evidence implicate the OPL in MFSD8-associated retinal disease. The localization of MFSD8 to the photoreceptor presynaptic terminals, together with the presence of a post-phototransduction ERG abnormality in patients with MFSD8 mutations, strongly suggests a synaptic origin for the defect. Synaptic alterations have previously been suggested as initiating events causing NCL in the CLN5-knockout sheep<sup>22</sup> and in a mouse model of lysosomal disease due to a defect in cathepsin D function (CLN10).<sup>23</sup>

Overall, the data suggest that macular photoreceptors appear to be most sensitive to mutations in MFSD8. Extramacular photoreceptors are the next most vulnerable, with cortical neurons being the most resistant of the affected cell types. There are anatomical and physiological differences between photoreceptor and conventional synapses that could account for this differential vulnerability. Photoreceptor terminals release neurotransmitter continuously, with light turning off vesicle release, whereas cortical neurons are usually switched off and are only triggered by action potentials. To permit these unique properties of photoreceptors, the terminals contain many more synaptic vesicles of which ~85% are freely mobile, actively participating in glutamate release, compared to ~20% in conventional synapses.<sup>24–27</sup> Furthermore, photoreceptor termini possess a synaptic ribbon for vesicle docking, necessary for maintaining the higher rates of neurotransmitter release over a sustained period of time.<sup>28</sup> It is also relevant that peripheral cones contain twice as many ribbons as central cones,<sup>29</sup> suggesting that this, or a similar synaptic modification, may underlie the different photoreceptor sensitivities.

To date, MFSD8 has been shown to be a lysosomal membrane protein with an MFS transporter domain that is characteristic of proteins that transport small solutes through chemiosmotic ion gradients.<sup>30</sup> The substrates for MFSD8 are unknown. However, as MFSD8 predominantly localizes to photoreceptor synaptic terminals in the retina, it could be speculated that it may form part of the synaptic vesicles. The consequences of MFSD8 mutation may be synaptic dysfunction resulting in disordered neurotransmitter release and local excitotoxicity. This may lead to downstream secondary consequences that have been described such as the accumulation of aggregate storage material in neuronal cells,<sup>5,16,31,32</sup> impaired autophagy,<sup>33</sup> and cell death, as well as accompanying inflammation that occurs both in the brains of MFSD8-deficient patients<sup>31</sup> and in the MFSD8-knockout dog<sup>34</sup> and mouse models.<sup>33,35</sup>

All previously published MFSD8 mutation combinations associated with disease are listed at <http://www.ucl.ac.uk/ncl/>

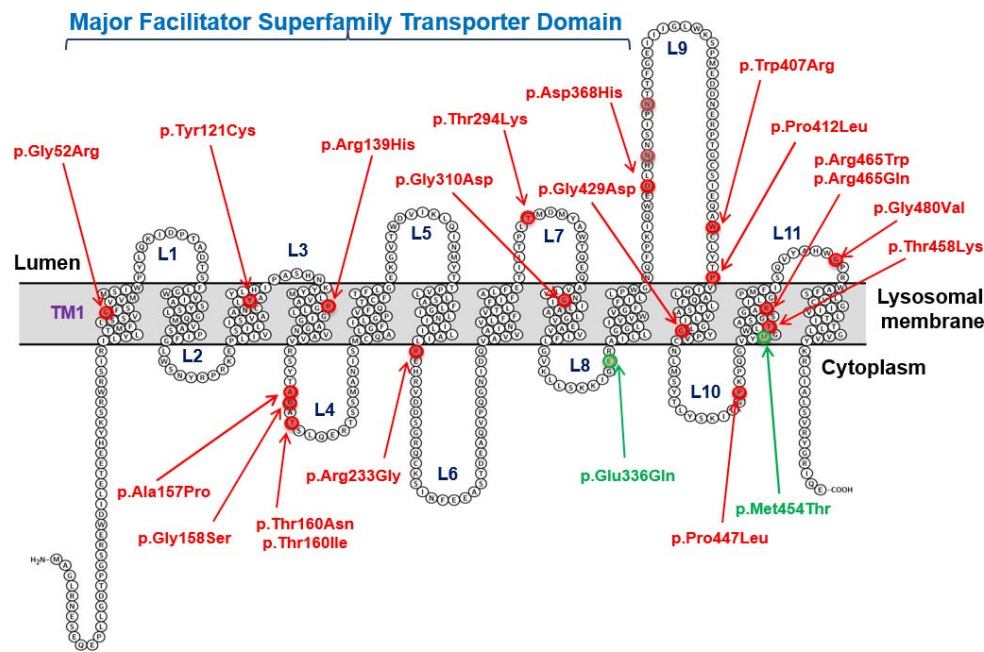


**FIGURE 5.** Topology prediction diagram of MFSD8 showing the location of pathogenic missense mutations. The 12 transmembrane protein spanning the lysosomal membrane was visualized at <http://wlab.ethz.ch/protter/> (provided in the public domain) using the protein sequence with accession code NP\_689991.1. The loops (L1–L11) on the luminal and cytoplasmic surfaces, as well as the MFS transporter domain motif, are highlighted. The two Asn-linked glycosylation residues in L9 are circled in *brown*. Residues that are affected in pathogenic missense mutations giving rise to vLINCL are depicted in *red*. Note that residues that are important in giving rise to nonsyndromic eye disease are highlighted in *green*.

CLN7patienttable.htm (provided in the public domain by the University College London, UK). The previously described p.Glu336Gln substitution, which gives rise to a “mild” variant allele, causes isolated macular dystrophy when paired either with a null variant on the other allele<sup>9</sup> or a missense variant (p.Arg465Gln) as shown here. In direct contrast, the p.Arg465Gln variant, when paired with a null allele, causes vLINCL rather than isolated retinal disease.<sup>14</sup> The other allele of interest, p.Met454Thr, may be considered a “moderate” allele since homozygous variants cause a more severe rod-cone dystrophy but not vLINCL. The severe neurological phenotype may only occur when the p.Met454Thr variant is paired with a more severe allele.<sup>17</sup> In addition, an atypical patient with late-onset vLINCL was homozygous for the p.Ala157Pro missense variant, suggesting that allele may be hypomorphic, accounting for the less severe phenotype.<sup>7</sup> All other reported cases with homozygous missense alleles cause vLINCL. A study that overexpressed two vLINCL-causing missense mutations, p.Thr294Lys and p.Pro412Leu, found enhanced proteolytic cleavage of mutant MFSD8 by cysteine proteases, inactivating the protein. It was suggested that some of the missense alleles may represent functional null mutations.<sup>36</sup> Based on the pathogenicity prediction scores of the missense mutations (Supplementary Table S2) and the topology prediction diagram that maps the mutations on the protein sequence (Fig. 5) there appears to be no obvious correlation between the mutations and whether the patient develops vLINCL or nonsyndromic eye disease. The missense changes, p.Glu336Gln and p.Met454Thr, that are associated with nonsyndromic eye disease may disrupt normal protein function either by reducing the transporter function of MFSD8 or by abrogating a yet to be defined specific function that is unique to photoreceptor synapses, but absent from conventional synapses.

To conclude, this study describes patients with isolated retinal disease due to biallelic mutations in *MFSD8*, a gene more usually associated with vLINCL. The data suggest a genotype/phenotype relationship such that a mild reduction in

function results in an isolated later-onset maculopathy; moderate reduction results in an earlier-onset generalized rod-cone dystrophy; and much wider central nervous system pathology if both alleles are functionally null. ERG demonstrates additional dysfunction occurring after phototransduction in the cone system, and immunofluorescence localizes the putative lysosomal transporter MFSD8 to the photoreceptor presynaptic terminals in the retinal OPL. Together these observations support a synaptic defect as the primary basis of pathology for this type of vLINCL and related diseases.

### Acknowledgments

Supported by grants from NERC (Yorkshire branch), the National Institute for Health Research (NIHR) for the NIHR BioResource–Rare Diseases project (RG65966), the Biomedical Research Centre at Moorfields Eye Hospital, the University College London Institute of Ophthalmology, Moorfields Eye Hospital Special Trustees, Foundation Fighting Blindness–USA, Research to Prevent Blindness–Casey Eye Institute, and RP Fighting Blindness and Fight For Sight (RP Genome Project GR586). Michel Michaelides is supported by an FFB Career Development Award, MEP by an FFB Enhanced Career Development Award, and KNK by an NIHR Rare Disease Fellowship.

Disclosure: **K.N. Khan**, None; **M.E. El-Asrag**, None; **C.A. Ku**, None; **G.E. Holder**, None; **M. McKibbin**, None; **G. Arno**, None; **J.A. Poulter**, None; **K. Carss**, None; **T. Bommireddy**, None; **S. Bagheri**, None; **B. Bakall**, None; **H.P. Scholl**, None; **F.L. Raymond**, None; **C. Toomes**, None; **C.F. Inglehearn**, None; **M.E. Pennesi**, None; **A.T. Moore**, None; **M. Michaelides**, None; **A.R. Webster**, None; **M. Ali**, None

### References

1. Mysore N, Koenekoop J, Li S, et al. A review of secondary photoreceptor degenerations in systemic disease. *Cold Spring Harb Perspect Med.* 2014;5:a025825.

2. Mole SE, Cotman SL. Genetics of the neuronal ceroid lipofuscinoses (Batten disease). *Biochim Biophys Acta*. 2015;1852:2237-2241.
3. Santavuori P. Neuronal ceroid-lipofuscinoses in childhood. *Brain Dev*. 1988;10:80-83.
4. Siintola E, Topcu M, Aula N, et al. The novel neuronal ceroid lipofuscinosis gene MFSD8 encodes a putative lysosomal transporter. *Am J Hum Genet*. 2007;81:136-146.
5. Aiello C, Terracciano A, Simonati A, et al. Mutations in MFSD8/CLN7 are a frequent cause of variant-late infantile neuronal ceroid lipofuscinosis. *Hum Mutat*. 2009;30:E530-E540.
6. Aldahmesh MA, Al-Hassnan ZN, Aldosari M, Alkuraya FS. Neuronal ceroid lipofuscinosis caused by MFSD8 mutations: a common theme emerging. *Neurogenetics*. 2009;10:307-311.
7. Kousi M, Siintola E, Dvorakova L, et al. Mutations in CLN7/MFSD8 are a common cause of variant late-infantile neuronal ceroid lipofuscinosis. *Brain*. 2009;132:810-819.
8. Stogmann E, El Tawil S, Wagenstaller J, et al. A novel mutation in the MFSD8 gene in late infantile neuronal ceroid lipofuscinosis. *Neurogenetics*. 2009;10:73-77.
9. Roosing S, van den Born LI, Sangermano R, et al. Mutations in MFSD8, encoding a lysosomal membrane protein, are associated with nonsyndromic autosomal recessive macular dystrophy. *Ophthalmology*. 2015;122:170-179.
10. Bach M, Brigell MG, Hawlina M, et al. ISCEV standard for clinical pattern electroretinography (PERG): 2012 update. *Doc Ophthalmol*. 2013;126:1-7.
11. McCulloch DL, Marmor MF, Brigell M, et al. ISCEV standard for full-field clinical electroretinography (2015 update). *Doc Ophthalmol*. 2015;130:1-12.
12. Koulen P, Fletcher EL, Craven SE, Brecht DS, Wässle H. Immunocytochemical localization of the postsynaptic density protein PSD-95 in the mammalian retina. *J Neurosci*. 1998;18:10136-10149.
13. Hirano AA, Brandstätter JH, Morgans CW, Brecha NC. SNAP25 expression in mammalian retinal horizontal cells. *J Comp Neurol*. 2011;519:972-988.
14. Kousi M, Lehesjoki AE, Mole SE. Update of the mutation spectrum and clinical correlations of over 360 mutations in eight genes that underlie the neuronal ceroid lipofuscinoses. *Hum Mutat*. 2012;33:42-63.
15. Santorelli FM, Garavaglia B, Cardona F, et al. Molecular epidemiology of childhood neuronal ceroid-lipofuscinosis in Italy. *Orphanet J Rare Dis*. 2013;8:19.
16. Mandel H, Cohen Katsanelson K, Khayat M, et al. Clinicopathological manifestations of variant late infantile neuronal ceroid lipofuscinosis (vLINCL) caused by a novel mutation in MFSD8 gene. *Eur J Med Genet*. 2014;57:607-612.
17. Patiño LC, Battu R, Ortega-Recalde O, et al. Exome sequencing is an efficient tool for variant late-infantile neuronal ceroid lipofuscinosis molecular diagnosis. *PLoS One*. 2014;9:e109576.
18. Craiu D, Dragostin O, Dica A, et al. Rett-like onset in late-infantile neuronal ceroid lipofuscinosis (CLN7) caused by compound heterozygous mutation in the MFSD8 gene and review of the literature data on clinical onset signs. *Eur J Paediatr Neurol*. 2015;19:78-86.
19. Di Fruscio G, Schulz A, De Cegli R, et al. Lysoplex: an efficient toolkit to detect DNA sequence variations in the autophagy-lysosomal pathway. *Autophagy*. 2015;11:928-938.
20. McBain VA, Egan CA, Pieris SJ, et al. Functional observations in vitamin A deficiency: diagnosis and time-course of recovery. *Eye*. 2007;21:367-376.
21. Sergouniotis PI, Sohn EH, Li Z, et al. Phenotypic variability in RDH5 retinopathy (fundus albipunctatus). *Ophthalmology*. 2011;118:1661-1670.
22. Amorim IS, Mitchell NL, Palmer DN, et al. Molecular neuropathology of the synapse in sheep with CLN5 Batten disease. *Brain Behav*. 2015;5:e00401.
23. Partanen S, Haapanen A, Kielar C, et al. Synaptic changes in the thalamocortical system of cathepsin D-deficient mice: a model of human congenital neuronal ceroid-lipofuscinosis. *J Neuropathol Exp Neurol*. 2008;67:16-29.
24. Pyle JL, Kavalali ET, Piedras-Rentería ES, Tsien RW. Rapid reuse of readily releasable pool vesicles at hippocampal synapses. *Neuron*. 2000;28:221-231.
25. Richards DA, Guatimosim C, Rizzoli SO, Betz WJ. Synaptic vesicle pools at the frog neuromuscular junction. *Neuron*. 2003;39:529-541.
26. Rea R, Li J, Dharia A, Levitan ES, Sterling P, Kramer RH. Streamlined synaptic vesicle cycle in cone photoreceptor terminals. *Neuron*. 2004;41:755-766.
27. Choi SY, Borghuis BG, Rea R, Levitan ES, Sterling P, Kramer RH. Encoding light intensity by the cone photoreceptor synapse. *Neuron*. 2005;48:555-562.
28. Sterling P, Matthews G. Structure and function of ribbon synapses. *Trends Neurosci*. 2005;28:20-29.
29. Chun MH, Grünert U, Martin PR, Wässle H. The synaptic complex of cones in the fovea and in the periphery of the macaque monkey retina. *Vision Res*. 1996;36:3383-3395.
30. Pao SS, Paulsen IT, Saier MH Jr. Major facilitator superfamily. *Microbiol Mol Biol Rev*. 1998;62:1-34.
31. Sharifi A, Kousi M, Sagné C, et al. Expression and lysosomal targeting of CLN7, a major facilitator superfamily transporter associated with variant late-infantile neuronal ceroid lipofuscinosis. *Hum Mol Genet*. 2010;19:4497-4514.
32. Jankowiak W, Brandenstein L, Dulz S, Hagel C, Storch S, Bartsch U. Retinal degeneration in mice deficient in the lysosomal membrane protein CLN7. *Invest Ophthalmol Vis Sci*. 2016;57:4989-4998.
33. Brandenstein L, Schweizer M, Sedlacik J, Fiehler J, Storch S. Lysosomal dysfunction and impaired autophagy in a novel mouse model deficient for the lysosomal membrane protein Cln7. *Hum Mol Genet*. 2016;25:777-791.
34. Guo J, O'Brien DP, Mhlanga-Mutangadura T, et al. A rare homozygous MFSD8 single-base-pair deletion and frameshift in the whole genome sequence of a Chinese Crested dog with neuronal ceroid lipofuscinosis. *BMC Vet Res*. 2015;10:960.
35. Damme M, Brandenstein L, Fehr S, et al. Gene disruption of Mfsd8 in mice provides the first animal model for CLN7 disease. *Neurobiol Dis*. 2014;65:12-24.
36. Steenhuis P, Froemming J, Reinheckel T, Storch S. Proteolytic cleavage of the disease-related lysosomal membrane glycoprotein CLN7. *Biochim Biophys Acta*. 2012;1822:1617-1628.

## APPENDIX

The NIH BioResource-Rare Diseases Consortium includes Timothy Aitman, Hana Alachkar, Sonia Ali, Louise Allen, David Allsup, Gautum Ambegaonkar, Julie Anderson, Richard Antrobus, Ruth Armstrong, Gavin Arno, Gururaj Arumugakani, Sofie Ashford, William Astle, Antony Attwood, Steve Austin, Chiara Bacchelli, Tamam Bakchoul, Tadbir K. Bariana, Helen Baxendale, David Bennett, Claire Bethune, Shahnaz Bibi, Maria Bitner-Glindzicz, Marta Bleda, Harm Boggard, Paula Bolton-Maggs, Claire Booth, John R. Bradley, Angie Brady, Matthew Brown, Michael Browning, Christine Bryson, Siobhan Burns, Paul Calleja, Natalie Canham, Jenny Carmichael, Keren Carss, Mark Caulfield, Elizabeth Chalmers, Anita Chandra, Patrick Chinnery, Manali Chitre, Colin Church, Emma Clement, Naomi Clements-Brod, Virginia Clowes, Gerry Coghlan, Peter Collins, Nichola Cooper, Amanda Creaser-Myers, Rosa DaCosta, Louise Daugherty, Sophie Davies, John Davis, Minka De Vries, Patrick



Deegan, Sri V.V. Deevi, Charu Deshpande, Lisa Devlin, Eleanor Dewhurst, Rainer Doffinger, Natalie Dormand, Elizabeth Drewe, David Edgar, William Egner, Wendy N. Erber, Marie Erwood, Tamara Everington, Remi Favier, Helen Firth, Debra Fletcher, Frances Flinter, James C. Fox, Amy Frary, Kathleen Freson, Bruce Furie, Abigail Furnell, Daniel Gale, Alice Gardham, Michael Gattens, Neeti Ghali, Pavandeep K. Ghatia, Rohit Ghurye, Simon Gibbs, Kimberley Gilmour, Paul Gissen, Sarah Goddard, Keith Gomez, Pavel Gordins, Stefan Gräf, Daniel Greene, Alan Greenhalgh, Andreas Greinacher, Sofia Grigoriadou, Detelina Grozeva, Scott Hackett, Charaka Hadinnapola, Rosie Hague, Matthias Haimel, Csaba Halmagyi, Tracey Hammerton, Daniel Hart, Grant Hayman, Johan W.M. Heemskerk, Robert Henderson, Anke Hensiek, Yvonne Henskens, Archana Herwadkar, Simon Holden, Muriel Holder, Susan Holder, Fengyuan Hu, Aarnoud Huissoon, Marc Humbert, Jane Hurst, Roger James, Stephen Jolles, Dragana Josifova, Rashid Kazmi, David Keeling, Peter Kelleher, Anne M. Kelly, Fiona Kennedy, David Kiely, Nathalie Kingston, Ania Koziell, Deepa Krishnakumar, Taco W. Kuijpers, Dinakantha Kumararatne, Manju Kurian, Michael A. Laffan, Michele P. Lambert, Hana Lango Allen, Allan Lawrie, Sara Lear, Melissa Lees, Claire Lentaigne, Ri Liesner, Rachel Linger, Hilary Longhurst, Lorena Lorenzo, Rajiv Machado, Rob Mackenzie, Robert MacLaren, Eamonn Maher, Jesmeen Maimaris, Sarah Mangles, Ania Manson, Rutendo Mapeta, Hugh S. Markus, Jennifer Martin, Larahmie Masati, Mary Mathias, Vera Matser, Anna Maw, Elizabeth McDermott, Coleen McJannet, Stuart Meacham, Sharon Meehan, Karyn Megy, Sarju Mehta, Michel Michaelides, Carolyn M. Millar, Shahin Moledina, Anthony Moore, Nicholas Morrell, Andrew Mumford, Sai Murng, Elaine Murphy, Sergey Nejentsev, Sadia Noorani, Paquita Nurden, Eric Oksenhendler, Willem H. Ouwehand, Sofia Papadia, Soo-Mi Park, Alasdair Parker, John Pasi, Chris Patch, Joan Paterson, Jeanette Payne, Andrew Peacock, Kathelijne Peerlinck, Christopher J. Penkett,

Joanna Pepke-Zaba, David J. Perry, Val Pollock, Gary Polwarth, Mark Ponsford, Waseem Qasim, Isabella Quinti, Stuart Rankin, Julia Rankin, F. Lucy Raymond, Karola Rehnstrom, Evan Reid, Christopher J. Rhodes, Michael Richards, Sylvia Richardson, Alex Richter, Irene Roberts, Matthew Rondina, Elisabeth Rosser, Catherine Roughley, Kevin Rue-Albrecht, Crina Samarghitean, Alba Sanchis-Juan, Richard Sandford, Saikat Santra, Ravishankar Sargur, Sinisa Savic, Sol Schulman, Harald Schulze, Richard Scott, Marie Scully, Suranjith Seneviratne, Carrock Sewell, Olga Shamardina, Debbie Shipley, Ilenia Simeoni, Suthesh Sivapalaratnam, Kenneth Smith, Aman Sohal, Laura Southgate, Simon Staines, Emily Staples, Hans Stauss, Penelope Stein, Jonathan Stephens, Kathleen Stirrups, Sophie Stock, Jay Suntharalingam, R. Campbell Tait, Kate Talks, Yvonne Tan, Jecko Thachil, James Thaventhiran, Ellen Thomas, Moira Thomas, Dorothy Thompson, Adrian Thrasher, Marc Tischkowitz, Catherine Titterton, Cheng-Hock Toh, Mark Toshner, Carmen Treacy, Richard Trembath, Salih Tuna, Wojciech Turek, Ernest Turro, Chris Van Geet, Marijke Veltman, Julie Vogt, Julie von Ziegenweldt, Anton Vonk Noordegraaf, Emma Wakeling, Ivy Wanjiku, Timothy Q. Warner, Evangeline Wassmer, Hugh Watkins, Andrew Webster, Steve Welch, Sarah Westbury, John Wharton, Deborah Whitehorn, Martin Wilkins, Lisa Willcocks, Catherine Williamson, Geoffrey Woods, John Wort, Nigel Yeatman, Patrick Yong, Tim Young, and Ping Yu.

The UK Inherited Retinal Disease Consortium includes Graeme Black, Georgina Hall, Stuart Ingram, Rachel Taylor, Simon Ramsden, Forbes Manson, Panagiotis Sergouniotis, Andrew Webster, Alison Hardcastle, Michel Michaelides, Vincent Plagnol, Michael Cheetham, Gavin Arno, Alessia Fiorentino, Nikolas Pontikos, Shomi Bhattacharya, Anthony Moore, Kamron Khan, Chris Inglehearn, Carmel Toomes, Manir Ali, Martin McKibbin, James Poulter, Emma Lord, Andrea Nemeth, Susan Downes, Stephanie Halford, Jing Yu, Stefano Lise, and Veronica van Heyningen.